Polymer Chemistry

ROYAL SOCIETY OF CHEMISTRY

PAPER

View Article Online
View Journal | View Issue

Cite this: *Polym. Chem.*, 2025, **16**, 3977

Soft block sulfonated styrene–butadiene–styrene (SBS) triblock copolymer proton exchange membranes

Michael K. Pagels,† Ding Tian,† Stefan Turan and Chulsung Bae *

Received 7th June 2025,
Accepted 3rd August 2025

DOI: 10.1039/d5py00569h

rsc.li/polymers

A new synthetic method that generates a middle block sulfonated SEBS proton exchange membrane through partial hydrogenation of polystyrene-*b*-polybutadiene-*b*-polystyrene and a subsequent thiol–ene click reaction and oxidation. By switching the sulfonation site from hard polystyrene end blocks to the soft poly(ethylene-*r*-butylene) middle block, the middle block sulfonated SEBS membranes showed lower swelling in water and greater dimensional stability than conventional polystyrene block sulfonated SEBSs with similar sulfonate concentrations because of the lack of the plasticization effect of the polystyrene block. Water uptake can be suppressed further by crosslinking unreacted carbon–carbon double bonds in the backbone after the thiol–ene click reaction by the addition of a photoacid. Crosslinked membranes showed good conductivity in water and resilient mechanical properties in stress–strain analysis.

Introduction

Proton exchange membranes (PEMs) are a class of ion-conducting polymer materials that have found use in a number of electrochemical energy conversion applications including fuel cells,[1,2] electrolyzers,[3,4] redox flow batteries,[5,6] (reverse) electrodialysis,[7,8] and electrochemical hydrogen compression.[9,10] In these systems, the PEM serves as a physical barrier while enabling selective transport of protons between the anode and cathode. Advancement in these ion-conducting materials is crucial for the development of reliable energy storage and conversion systems from renewable energy sources and, ultimately, reducing the release of carbon dioxide into the environment. Perfluorosulfonic acid polymers, such as Nafion, have been used as standard PEM materials for these applications due to their exceptional chemical stability and efficient transport of ions. There is, however, a need to develop high-performing hydrocarbon PEMs from commodity materials for use in applications that do not require high chemical and oxidative stability such as electrodialysis and electrochemical hydrogen compression. The switch from Nafion to hydrocarbon PEMs could be a key factor in lowering the device cost with the added benefit of reducing potential release of environmentally persistent and toxic perfluoroalkyl substances from the production and degradation of Nafion.[11]

Polystyrene-*b*-poly(ethylene-*r*-butylene)-*b*-polystyrene (SEBS, Fig. 1a) is a well-known and widely available thermoplastic triblock copolymer exhibiting microphase separated morphologies at the nanoscale due to the incompatibility between the covalently bound polystyrene end blocks and poly(ethylene-*r*-butylene) middle block.[12] In this system, the higher T_g (~100 °C) polystyrene end block provides mechanical strength to SEBS by means of physical crosslinking, while the rubbery poly(ethylene-*r*-butylene) middle block provides elasticity, preventing the material from fracture. The nanophase separated morphology created from the "hard" and "soft" blocks can be advantageous for PEM applications since such a morphology can deliver elastic and tough membrane materials with a low tendency to crack under mechanical stress. Furthermore, selective functionalization of one of these blocks can yield high local charge density polymers with ionically conductive channels and mechanically resilient properties. SEBS has previously been used in the preparation of PEMs but they have mainly consisted of styrene block functionalization through electrophilic sulfonation using sulfuric acid, acetyl sulfate or chlorosulfonic acid (Fig. 1a).[13–15] This material design has the advantage of convenient installation of sulfonates to the aromatic rings of the polystyrene block of SEBS.[16] When it is hydrated, however, water molecules near the sulfonate functionality act as a plasticizer and disrupt the physical crosslinks of the polystyrene block, causing uncontrolled swelling and poor mechanical strength.

Department of Chemistry & Chemical Biology, Rensselaer Polytechnic Institute, Troy, New York 12180, USA. E-mail: baec@rpi.edu
† These authors contributed equally to this work.

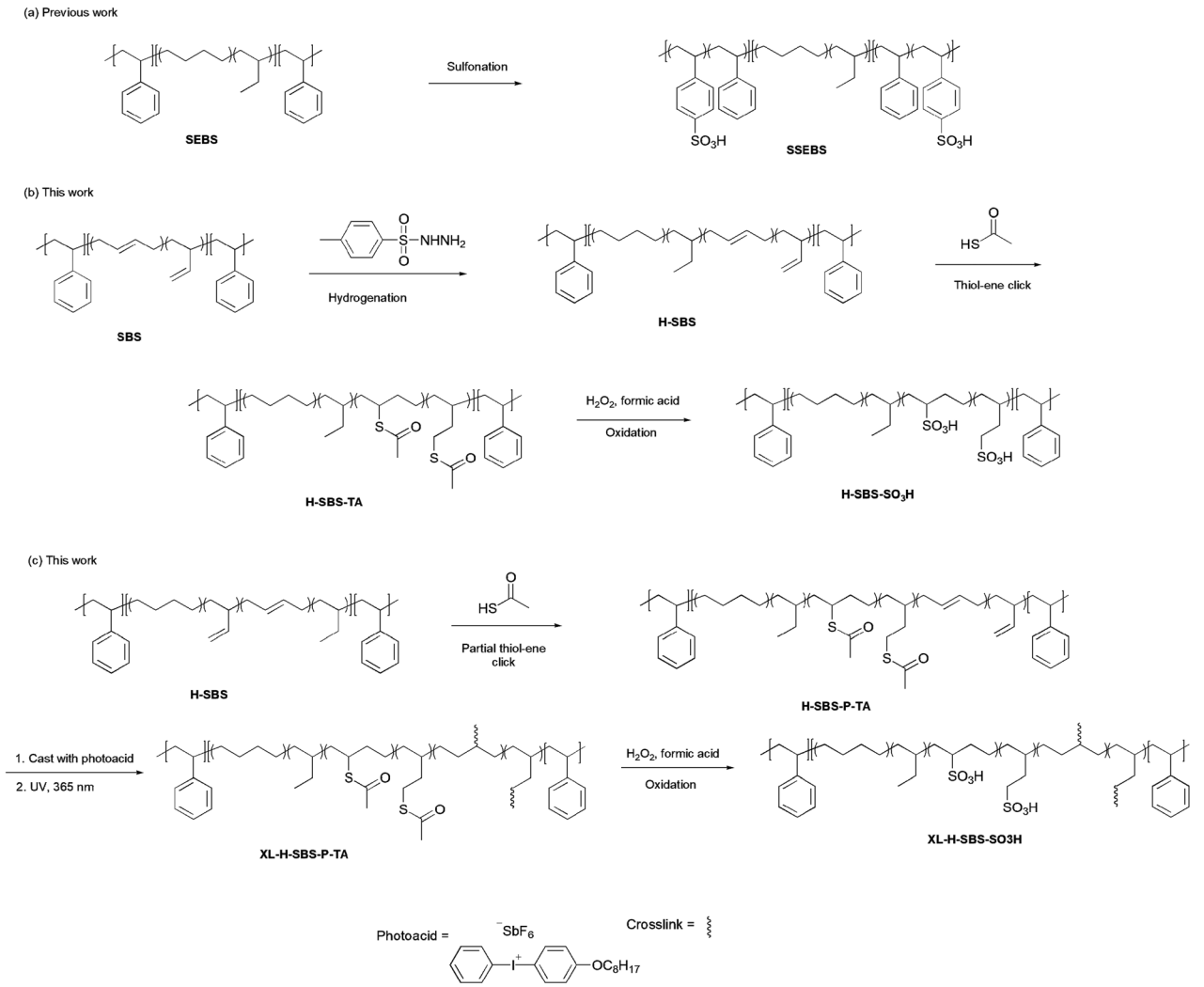

Fig. 1 Synthesis of SEBS polymers with (a) styrene block sulfonation, (b) middle block sulfonation, and (c) middle block sulfonation and crosslinking.

In this work, we propose the synthesis of hydrocarbon triblock copolymer PEMs with functionalization at the middle block of SEBS. Sulfonation in the middle soft polymer block would suppress water uptake and better preserve the mechanical integrity of the block copolymer PEMs. Furthermore, we introduce a novel UV-induced crosslinking method that can serve as a valuable tool to further control water uptake of high ion exchange capacity (IEC) membranes.

Experimental

Materials

SBS (31/69 wt% (*i.e.*, 19/81 mol%) styrene/butadiene, Kraton D1192 ET), *p*-toluenesulfonyl hydrazide (98%, Alfa Aesar), tripropylamine (98%, Acros Organics), thioacetic acid (98%, Acros Organics), benzophenone (99%, Alfa Aesar), butylated hydroxytoluene (BHT, 99%, Sigma Aldrich), formic acid (99%, Acros Organics), hydrogen peroxide (30 wt% in water, EMD Millipore), (4-(octyloxy)phenyl)(phenyl)iodonium hexafluorostibate(v) (97%, Millipore Sigma), anhydrous toluene (99.85%, Acros Organics), tetrahydrofuran (THF, 99%, Honeywell), and $CDCl_3$ (99.96% D, Cambridge Isotope Laboratories) were used as received.

Partial hydrogenation of SBS

The synthesis of H-SBS-9.2 (where the suffix represents the mole percentage of the remaining double bonds) will be used as an example. To a 500 mL 2-neck round bottom flask, SBS (5.0 g, 78.7 mmol SBS repeating unit with 63 mmol of C=C bonds), *p*-toluenesulfonyl hydrazide (13.6 g, 73.1 mmol) and toluene (200 mL) were added. The flask was fitted with a condenser and a rubber septum and purged with dry nitrogen. The solution was heated to reflux and then tripropylamine (10.4 g, 13.9 mL, 73.1 mmol) was added *via* a syringe. The reaction was refluxed for 6 h after addition of tripropylamine. It was then allowed to cool to room temperature after which the

polymer was precipitated into approximately 600 mL of methanol and recovered by vacuum filtration. The polymer was then dissolved in 100 mL of THF and again precipitated into approximately 300 mL of methanol. The polymer was obtained by vacuum filtration and vacuum drying at 60 °C overnight. 5.1 g, 99% yield. H-SBS-12.9, H-SBS-15.9, H-SBS-22.0, and H-SBS-39.3 were prepared using the same procedure and by adjusting the feed ratio of *p*-toluenesulfonyl hydrazide and tripropylamine.

Thiol–ene click reaction

The synthesis of H-SBS-TA-8.9 will be used as an example. To a 1000 mL 1-neck round bottom flask, H-SBS-9.2 (5.0 g, 5.74 mmol of the remaining C=C bonds), benzophenone (140.2 mg, 0.77 mmol), and anhydrous toluene (500 mL) were added. The flask was fitted with a septum and dry nitrogen gas was bubbled through the solution for 45 min. Thioacetic acid (2 equiv. with respect to residual C=C bonds in the polymer, 0.9 g, 0.81 mL, 11.5 mmol) was then added *via* a syringe. The solution was bubbled for an additional 15 min and then placed under UV light (365 nm, 8 W) with stirring for 4 h. The reaction was quenched by addition of BHT (approximately 50 mg) and the polymer was precipitated into 1500 mL of methanol. The polymer was vacuum filtered and dissolved in 100 mL of THF, and then precipitated again into 300 mL of methanol. The polymer was obtained by vacuum filtration and vacuum drying at 60 °C overnight. 5.5 g, 95% yield. Other H-SBS-TA samples were prepared using the same procedure.

Partial thiol–ene click reaction (H-SBS-P-TA-20.7)

The reaction follows the same procedure as the thiol–ene click reaction using H-SBS-39.3 (5.0 g, 26.7 mmol of the remaining C=C bonds), benzophenone (141 mg, 0.78 mmol), thioacetic acid (0.5 equiv. with respect to residual C=C bonds, 0.9 g, 0.88 mL, 12.3 mmol). 5.5 g, 92% yield.

Membrane casting

H-SBS-TA polymers were solution cast using toluene at 5 wt/v% concentration. The solutions were filtered through a short plug of silica to remove dust particles prior to casting. The freshly filtered solutions were then poured onto a glass plate and covered for slow evaporation of toluene. The samples were left to dry at room temperature overnight. The membranes were removed from the glass plate by immersing in methanol.

To cast H-SBS-P-TA, 1 mol% of photoacid with respect to the remaining carbon–carbon double bonds was added and aluminum foil was used to prevent light exposure while casting. The cast film was not rinsed with methanol until after crosslinking using UV light (365 nm, 300 W) for two minutes.

Sulfonation of membranes (H-SBS-SO_3H and XL-H-SBS-SO_3H)

The cast membranes of H-SBS-TA and XL-H-SBS-TA were immersed in a solution mixture of water, formic acid, and hydrogen peroxide in a 4 : 1 : 1 ratio at 50 °C, respectively. The membranes were oxidized at this temperature for 6 h and then rinsed thoroughly with fresh deionized water. The membranes were then placed in 1 M H_2SO_4 solution for 24 h, again washed thoroughly with deionized water, and then placed in fresh deionized water for 24 h. The membranes were then dried in a vacuum oven at 60 °C overnight to obtain the final sulfonated PEMs.

Gel fraction

To test the effectiveness of crosslinking, the XL-H-SBS-P-TA membrane was massed and then submerged in toluene for 24 h. Then the membranes were rinsed with fresh toluene followed by methanol. After drying in a vacuum at 60 °C overnight, the membranes were massed once more, and the gel fraction was calculated as follows:

$$\text{Gel fraction}\,(\%) = \frac{W_1}{W_2} \times 100$$

where W_2 is the mass before submerging in toluene and W_1 is the mass after submerging in toluene.

Membrane characterization

^{1}H NMR spectra were recorded with a Varian Unity 500 MHz spectrometer, and chemical shifts were referenced to the residual solvent peak ($CDCl_3$, δ 7.26 ppm). FT-IR spectra were recorded using a Nicolet (Thermo) 4700 FT-IR with a PIKE ZnSE/Diamond ATR accessory. Average molecular weights of the polymers were obtained by size exclusion chromatography on a Viscotek T60A instrument using THF as an eluent and polystyrene standards with a differential refractive index detector (Viscotek 302). Tensile strength testing was done using a TA Instruments Q800 with a DMA-RH accessory for humidity conditions. The size of membranes used for tensile strength measurement was approximately 20 mm × 5 mm × 0.05 mm.

Ion exchange capacity (IEC) was determined (a) from ^{1}H NMR spectra analysis of the precursor H-SBS-TA polymers (NMR IEC) and (b) by titration of the sulfonated polymers H-SBS-SO_3H and XL-H-SBS-SO_3H (titration IEC). To conduct IEC titration, membranes (~100 mg) in –SO_3H form were massed and then submerged in approximately 25 mL of 1 M NaCl for 24 h. The solution was then added into a flask, and the membrane was washed with approximately 3 mL of 1 M NaCl solution three times and again placed in the flask. This solution was then titrated using phenolphthalein as an indicator with freshly standardized 0.01 M NaOH. IEC calculation is as follows:

$$\text{IEC}\,(\text{mmol g}^{-1}) = \frac{V_{\text{NaOH}} \times C_{\text{NaOH}}}{W_{\text{d}}}$$

where V_{NaOH} is the volume of NaOH used in the titration, C_{NaOH} is the concentration of NaOH, and W_{d} is the dry mass of the membrane.

Water uptake was determined by the difference in the dry and wet mass of the membranes in proton form. Dry membranes of approximately 100 mg were massed and then placed in water for 24 h. The membranes were removed from water and then surface water was removed using a Kimwipe and quickly massed. An average of three samples was used to deter-

mine the water uptake. Calculation for water uptake is as follows:

$$\text{Water uptake}\,(\%) = \frac{W_w - W_d}{W_d} \times 100$$

where W_w and W_d are the wet and dry masses of the membranes, respectively.

The swelling ratio was measured similarly by measuring the dimensional change of the membranes from the dry to the wet state. The calculation is as follows:

$$\text{Swelling ratio}\,(\%) = \frac{L_w - L_d}{L_d} \times 100$$

where L_w and L_d are the wet and dry masses of the membranes, respectively.

The hydration number (λ) gives the moles of water per sulfonate group. The calculation for λ is as follows:

$$\lambda = \frac{\text{WU}}{100} \times \frac{1000}{18 \times \text{IEC}}$$

where WU is the water uptake.

Proton conductivity was measured in-plane in liquid water using the four-point probe method. Conductivity was measured using a BT-512 membrane conductivity test system (BekkTech LLC) by scanning direct current sweep from 0.1 V to −0.1 V and the linear voltage–current data are fitted to obtain the resistance. Conductivity (σ) is calculated as follows:

$$\sigma = \frac{L}{AR}$$

where L is the length between the two inner probes on the test cell, A is the cross-sectional area of the membrane, and R is the resistance (in liquid water).

Results and discussion

To demonstrate our new synthetic strategy for middle block sulfonated triblock copolymer PEMs, polystyrene-*b*-butadiene-*b*-styrene (SBS, Fig. 1b), which is the precursor polymer of SEBS, was partially hydrogenated (H-SBS) and the remaining carbon–carbon double bonds were reacted by means of a thiol–ene click reaction using thioacetic acid (H-SBS-TA). The membrane was then oxidized under heterogeneous conditions to give sulfonated polymer H-SBS-SO_3H (Fig. 1b). For the synthesis of a crosslinked sulfonated polymer, a novel crosslinking step was added to this scheme by leveraging the carbon–carbon double bonds of H-SBS. After the partial thiol–ene click reaction, the remaining C=C bonds of H-SBS-P-TA were crosslinked with a photoacid in film form (XL-H-SBS-P-TA). Oxidation of the thioacetate group in the crosslinked membrane using a mixture of H_2O_2 and formic acid produced its crosslinked sulfonated polymer membrane XL-H-SBS-SO_3H (Fig. 1c).

The C=C bonds in SBS (31/69 wt% styrene/butadiene) were partially hydrogenated by hydrazine generated *in situ* from *p*-toluenesulfonyl hydrazide[17] to give H-SBS-*x* (Fig. 1b), where *x* represents the mole percentage of the remaining C=C bonds in the polymer after hydrogenation, calculated from the change in integration of double bond peaks in ^{1}H NMR. The partial hydrogenation of SBS is necessary to control the IEC of the final sulfonated polymer and avoid leaving residual double bonds in the polymer, which can undergo side reactions in later steps. A series of five polymers with varying degrees of hydrogenation from 61 to 91% of total double bonds hydrogenated were synthesized (H-SBS-39.3, -22.0, -15.9, -12.9, and -9.2 as listed in Table 1). Next, a thiol–ene click reaction was performed to attach a thioacetate functionality to the ethylene/butadiene middle block of the polymer.[18] The thiol–ene click reaction is a versatile tool to economically incorporate functionality into polymeric systems.[19,20] The thiol–ene click reaction proceeded smoothly under UV light irradiation (365 nm, 8 W) using benzophenone as a radical initiator and produced thioacetate-functionalized polymer H-SBS-TA-*y* (where *y* represents the mole percentage of the thioacetate group incorporated into the polymer, calculated from integration of the thioacetate CH_3 peak in ^{1}H NMR). The FT-IR and ^{1}H NMR spectra of H-SBS-TA are given in Fig. 2, 3, and Fig. S1, and they match well with the expected chemical structures of the polymers.

SBS is commercially synthesized by anionic polymerization of styrene and butadiene, which affords the triblock polymer with a low dispersity ($Đ$). To study the effect of functionalization reactions on the molecular weights of the polymers, we analyzed number average molecular weights and dispersity with size exclusion chromatography (SEC) and the results are shown in Table 1 and Fig. S2. After hydrogenation, H-SBS showed a slight decrease in molecular weights due to a decrease in the hydrodynamic volume from the conversion of double bonds to saturated alkyl chains. After the thiol–ene click reaction, the M_n and dispersity of H-SBS-TA slightly increased, possibly caused by a small amount of coupling reactions between polymer chains.

Two types of side reactions that can occur in the radical addition of thioacetate are illustrated in Fig. 4; while an intra-

Table 1 Properties of H-SBS and H-SBS-TA

Sample	Residual C=C or thioacetate[a] (mol%)	M_n [b] (kg mol^{-1})	$Đ$[b]	C=C side reaction[c] (mol%)
SBS	100	134	1.13	—
H-SBS-9.2	9.2	117	1.25	—
H-SBS-12.9	12.9	122	1.20	—
H-SBS-15.9	15.9	116	1.16	—
H-SBS-22.0	22.0	112	1.17	—
H-SBS-39.3	39.3	109	1.18	—
H-SBS-TA-8.9	8.9	120	1.74	0.31
H-SBS-TA-12.3	12.3	126	1.31	0.54
H-SBS-TA-15.0	15.0	122	1.31	0.84
H-SBS-TA-20.0	20.0	148	1.18	1.95
H-SBS-P-TA-20.7	20.7	85	8.98	3.45

[a] Calculated from relative ^{1}H NMR integrations. [b] Calculated from SEC. [c] Calculated from the difference in relative integration of the loss of C=C and the appearance of a thioacetate CH_3 peak in ^{1}H NMR.

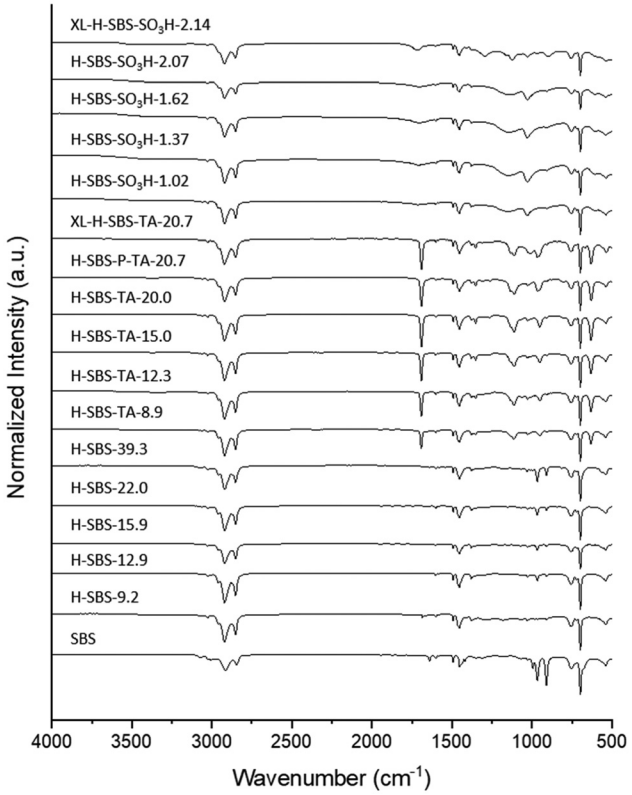

Fig. 2 FT-IR spectra of polymers.

molecular side reaction produces a cyclized ring in polymer chains (Fig. 4b), an intermolecular side reaction induces polymer chain couplings (Fig. 4c).[21] The last column of Table 1 lists the mole percentage of double bonds participating in the cyclization or interchain coupling side reactions, as measured by ^{1}H NMR spectroscopy. As the concentration of residual double bonds in H-SBS increased in the thiol–ene click reaction, the amount of side reactions in carbon–carbon double bonds gradually increased. A partial thiol–ene click reaction was conducted for H-SBS-39.3 to give H-SBS-P-TA-20.7, in which the residual double bonds were crosslinked after film formation. Unfortunately, this partial thiol–ene reaction experienced significant side reactions. The SEC traces of H-SBS-P-TA-20.7 show a significant shoulder towards shorter elution times, indicating a higher fraction of high molecular weight chains. Although this side reaction from the thiol–ene reaction cannot be completely avoided, all other thioacetate-functionalized polymers maintained a dispersity below 1.74, as shown in Fig. S2 and Table 1.

To test the effectiveness of the photoacid (structure given in Fig. 1c) in the crosslinking of these polymer systems, SBS was cast into a film with varying degrees of the photoacid (0.01 to 5 mol% with respect to C=C bonds) and irradiated with UV for 2 minutes to initiate crosslinking. The general mechanism of photoacid-induced crosslinking of SBS is illustrated in Fig. 5.[22,23] The effectiveness of crosslinking by this method was quantified by measuring the gel fraction of these polymers in toluene. The gel fraction results of Fig. 6 indicate that only a small amount of photoacid is necessary to create an insoluble polymer membrane. Similarly, 1 mol% loading of photoacid was sufficient for crosslinking of H-SBS-P-TA-20.7; after curing with UV irradiation, the gel fraction of XL-H-SBS-p-TA-20.7 was over 90% (Fig. 6).

To convert the thioester functionality in H-SBS-TA and XL-H-SBS-TA materials to –SO_3H form, they were oxidized

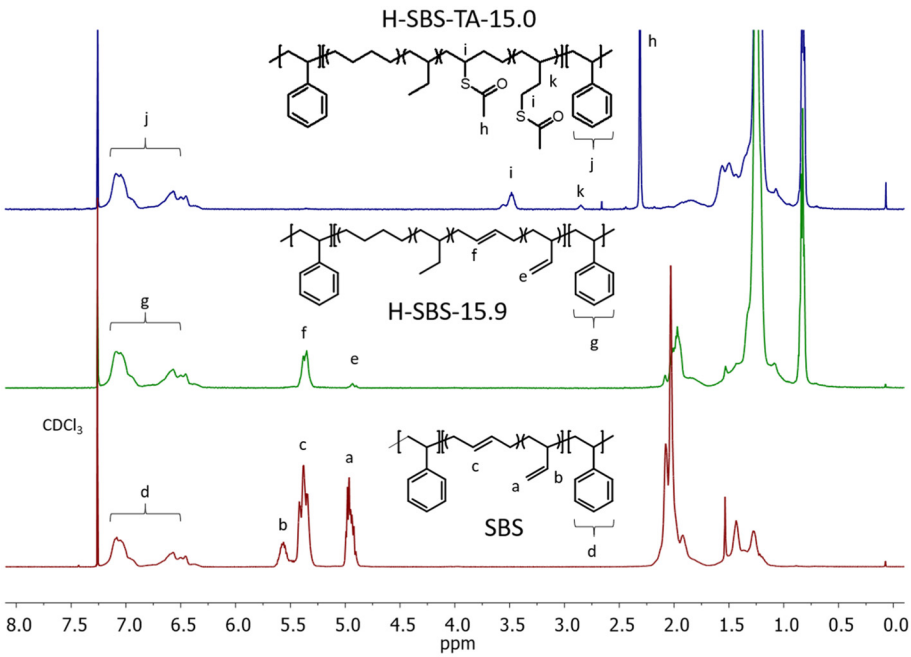

Fig. 3 ^{1}H NMR spectra of SBS (red), H-SBS-15.9 (green), and H-SBS-TA-15.0 (blue).

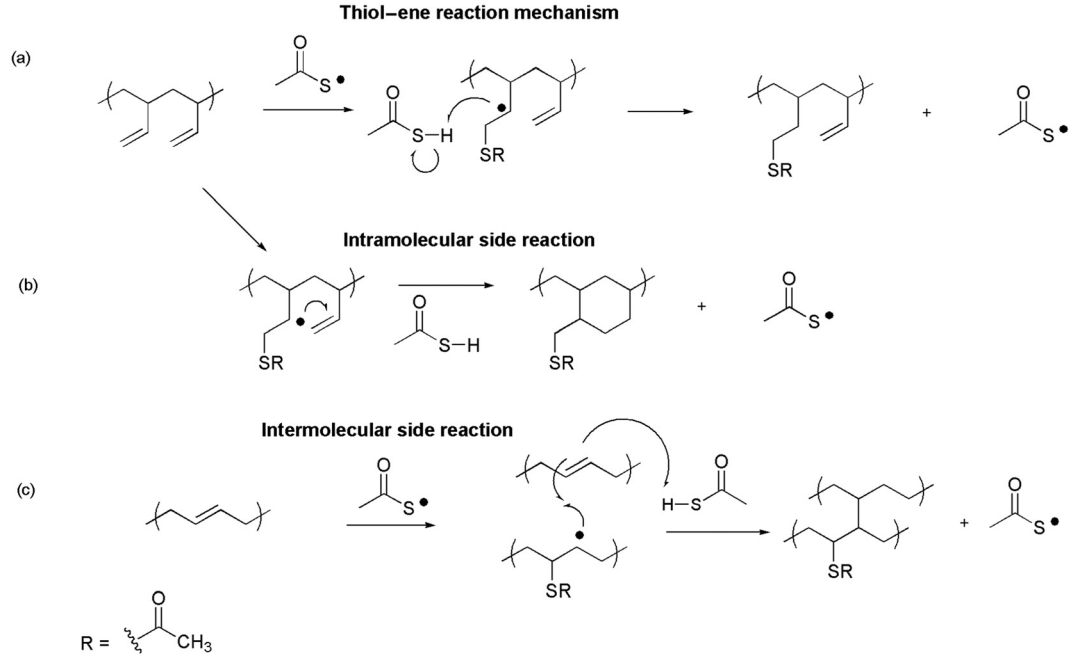

Fig. 4 (a) Thiol–ene click reaction mechanism, and (b and c) illustration of side reactions that account for a loss of double bonds and for an increase in polymer molecular weight and dispersity.

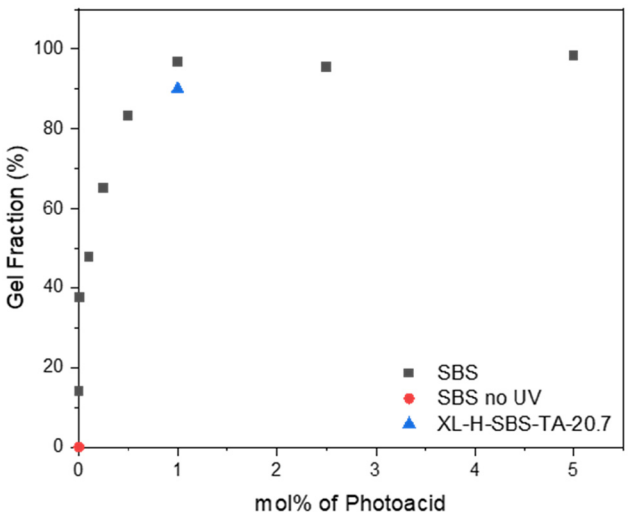

Fig. 5 Mechanism of photoacid crosslinking in membrane form.

heterogeneously in membrane form using a mixture of water, formic acid, and hydrogen peroxide in a 4 : 1 : 1 volume ratio.[18,24] We chose to perform heterogeneous oxidation for both thioester polymers because even uncrosslinked H-SBS-SO_3H was found to be insoluble once the thioacetate functionality of H-SBS-TA was converted to –SO_3H (and –SO_3Na) form; it is quite common to observe poor solubility (or no solubility) of sulfonated SBS and SEBS polymers, particularly those with high molecular weights, due to the lack of solvent composition that can dissolve both non-ionic polymer and sulfonated ionic polymer chains simultaneously. Thus, we utilized FT-IR spectroscopy to confirm complete conversion of the thioacetate functionality to sulfonic acid form in H-SBS-SO_3H and XL-H-SBS-SO_3H (Fig. 2). Note that the suffixes of the thioester polymers and those of sulfonated polymers in Fig. 2 have different meanings; while the suffix of thioester polymers indicates the mole percentage of the thioester functionality relative to the initial carbon–carbon double bonds

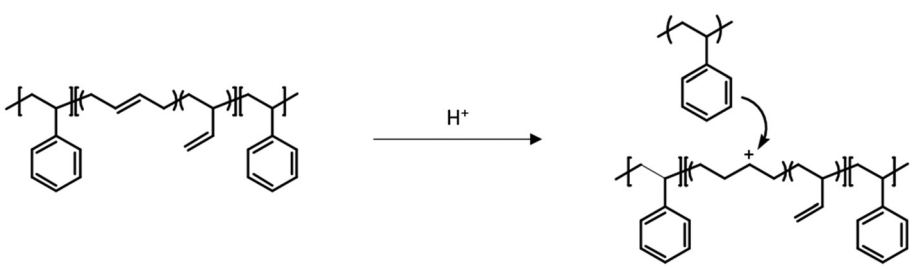

Fig. 6 Gel fraction of crosslinked polymers.

obtained from their ^{1}H NMR spectra (listed in Table 1), the suffix of sulfonated polymers indicates their corresponding IEC values with the assumption of complete conversion to sulfonate form (NMR IEC in Table 2). After the oxidation, the disappearance of the carbonyl peak at 1680 cm^{-1} indicates complete conversion to the sulfonate group in the polymer membranes. Successful oxidation of thioacetate to sulfonate was also confirmed using titration IECs, which match closely with the theoretical IECs calculated from the ^{1}H NMR spectra of H-SBS-TA precursors (Table 2).

The properties of H-SBS-SO_3H and crosslinked XL-H-SBS-SO_3H membranes were evaluated with respect to the IEC, water uptake and swelling ratio (Table 2). As the IEC of H-SBS-SO_3H increases, both water uptake and swelling ratios increase as a result of enhanced hydrophilicity from additional sulfonic acid groups in the polymer. There is a sharp increase in water uptake as the IEC_{NMR} increases from 1.37 to 1.62 mmol g^{-1} (more than three times) and excessive water uptake was seen for the H-SBS-SO_3H-2.07 material with an IEC of 2.07 mmol g^{-1}. For aliphatic hydrocarbon backbone-based PEMs, such as sulfonated SBS and SEBS, the IEC of membranes is generally limited to less than 2.0 mmol g^{-1} because of excessive water uptake caused by greater chain mobility when compared to ionic polymers made of an aromatic backbone.[16]

Despite the high water uptake of H-SBS-SO_3H membranes, when their water absorption properties were compared with those of polystyrene block sulfonated SEBS[14] (both in uncrosslinked systems), these soft middle block sulfonated membranes do show more restricted hydration numbers (λ, molar ratio of H_2O/SO_3^-), as graphically illustrated in Fig. 7. Similar to our recent study of SBS AEMs,[29,30] this lower water absorption behavior stems from the preservation of physical crosslinking at the styrene end blocks of SBS/SEBS. In the case of XL-H-SBS-SO_3H-2.14, the photo-initiated crosslinking reaction substantially reduced the chain mobility of the sulfonated middle block's ability to further prevent excess water uptake and suppress membrane swelling (blue triangle in Fig. 7).

The proton conductivity of H-SBS-SO_3H membranes was measured in water at 25 and 80 °C (Fig. 8). There is an increase in the conductivity from 25 °C to 80 °C when the IEC increases from 1.04 to 1.62 mmol g^{-1}. However, the H-SBS-SO_3H-2.07 membrane experienced excessive water

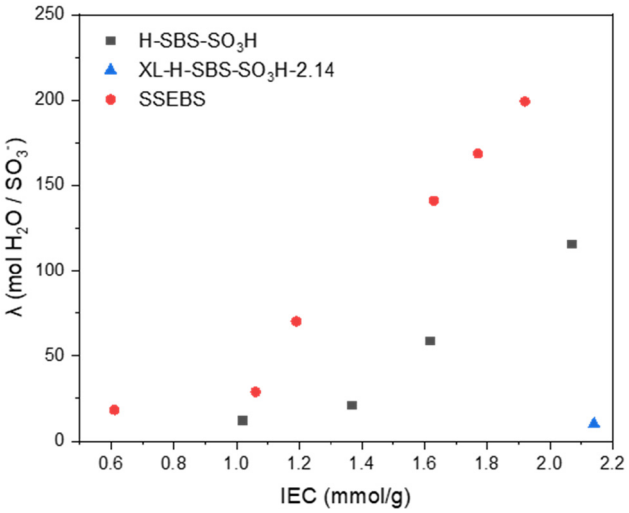

Fig. 7 Comparison of hydration numbers (λ) in styrene block sulfonation of SEBS (red) and middle block sulfonation of SEBS (black, H-SBS-SO_3H).

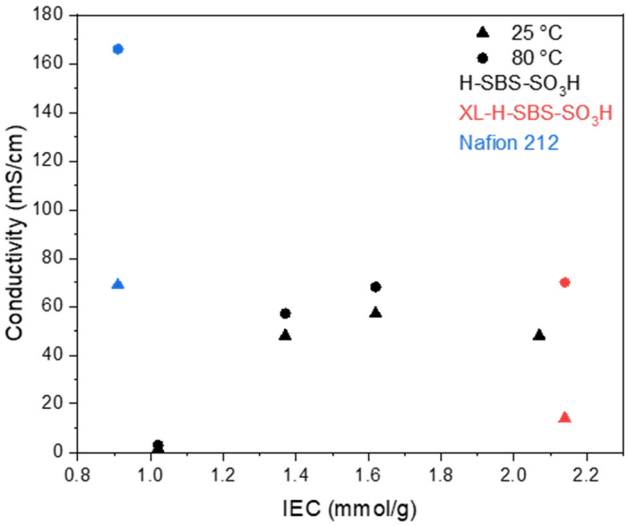

Fig. 8 Conductivity at 25 °C (circle) and 80 °C (triangle) of H-SBS-SO_3H (black), XL-H-SBS-SO_3H-2.14 (red) and Nafion 212 (blue).

Table 2 Properties of H-SBS-SO_3H membranes

Sample	NMR IEC[a] (mmol g^{-1})	Titration IEC[b] (mmol g^{-1})	Water uptake[c] (%)	Hydration number, λ (mol H_2O/SO_3^-)	Swelling ratio[c] (%)
H-SBS-SO_3H-1.02	1.02	0.75	21.5	11.7	9.3
H-SBS-SO_3H-1.37	1.37	1.19	51.2	20.8	12.1
H-SBS-SO_3H-1.62	1.62	1.48	170.8	58.6	23.8
H-SBS-SO_3H-2.07	2.07	1.82	430.3	115.5	40.5
XL-H-SBS-SO_3H-2.14	2.14	1.89	38.7	10.0	11.2

[a] Calculated from the ^{1}H NMR spectra of H-SBS-TA polymers. [b] Measured by acid–base titration. [c] Measured at room temperature in proton form.

Table 3 Conductivity and water normalized conductivity

	Conductivity, σ (mS cm^{-1})		σ/λ ratio	
Sample	25 °C	80 °C	25 °C	80 °C
H-SBS-SO_3H-1.02	1.5	3	0.13	0.26
H-SBS-SO_3H-1.37	48	57	2.31	2.74
H-SBS-SO_3H-1.62	57	68	0.97	1.16
H-SBS-SO_3H-2.07	48	—	0.41	—
XL-H-SBS-SO_3H-2.14	14	70	1.4	7.00

uptake, and the conductivity of this membrane could not be measured at 80 °C. On the other hand, the crosslinked XL-H-SBS-SO_3H-2.14 membrane showed good conductivity at 80 °C due to its lower swelling and better mechanical stability.

To understand the effective use of water in these membranes, the ratio of proton conductivity to hydration number is used as a metric (Table 3). A high ratio of conductivity to hydration number would be beneficial for electrochemical device applications since less water absorption can reduce the permeation of gaseous reactants and products of electrochemical reactions, such as H_2 in fuel cells and water electrolyzers, while still providing good ion conductivity. In vanadium redox flow batteries, the conductivity of protons to and from electrodes is important to reduce ohmic losses in charge and discharge operations while vanadium ion crossover across the membrane separator is detrimental to energy efficiency. Water uptake is a key parameter that dictates vanadium ion crossover where higher water uptake membranes tend to show higher vanadium crossover.[25,26] Similarly under humidified conditions, higher water content leads to higher gas permeability since most gas transport occurs through the water phase of the membrane, which can diminish cell performance and reduce efficiencies for fuel cells, electrolyzers, and electrochemical hydrogen compressor applications.[27,28] When the ratios of proton conductivity at 80 °C to the hydration numbers of the H-SBS-SO_3H-1.37 and XL-H-SBS-SO_3H-2.14 membranes are compared, the uncrosslinked membrane has a ratio of 2.74 while the crosslinked membrane has a ratio of 7.00 (see Table 3), indicating more efficient use of water within the membrane, suppressing excess swelling of the membrane while achieving high proton conductivity.

The mechanical properties of the middle block sulfonated SBS membranes were tested by stress–strain analysis at 50 °C under humidified and dry conditions (Fig. 9). All uncrosslinked membranes did not break until they reached the end of the limits of the DMA (300% strain). Due to the presence of an effectively crosslinked network, the XL-H-SBS-SO_3H-2.14 membrane showed the lowest strain at break among all samples tested; however, its maximum strain value is still greater than 100% under both humidified and dry conditions. Showing similar maximum strain values under different humidity conditions suggests that this strain value could be related to the unique polymer network structure such as crosslinking density. The decrease in tensile stress value of the crosslinked membrane at 50% relative humidity clearly illustrates the water plasticization effect on the poly(ethylene-*r*-butylene) middle block, though not as significant as that of the polystyrene end block, as we do not expect such an effect under dry conditions.

Conclusion

In conclusion, sulfonation of SBS to achieve a middle block sulfonated SEBS membrane is an effective means to produce proton exchange membranes from commodity materials. By moving the sulfonation site from the hard polystyrene end blocks to the soft poly(ethylene-*r*-butylene) middle block, greater preservation of the physical crosslinks created by the nano-scale phase separation in SEBS films was achieved because water does not plasticize the polystyrene hard blocks. This effect was shown by a decrease in water uptake compared to the polystyrene block sulfonated SEBS with comparable ion concentrations (IECs). Furthermore, the water uptake can be suppressed further by crosslinking unreacted carbon–carbon double bonds in the backbone after the thiol–ene click reaction by the addition of a photoacid. Ultimately, these (XL-)

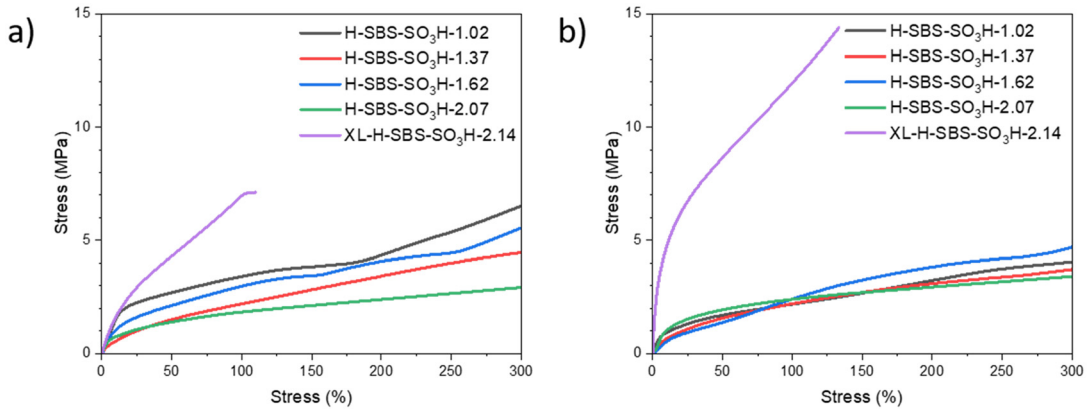

Fig. 9 Tensile stress–strain curves of sulfonated membranes under (a) 50 °C and 50% RH and (b) 50 °C and 0% RH conditions.

H-SBS-SO_3H membranes showed good conductivity in water and resilient mechanical properties shown through stress–strain analysis, providing a low-cost and convenient means to produce proton exchange membranes for electrochemical device applications.

Author contributions

Michael K. Pagels, Ding Tian, and Stefan Turan: methodology, formal analysis, data curation, writing – original draft preparation and writing – review & editing. Chulsung Bae: conceptualization, funding acquisition, supervision, and writing – review & editing.

Conflicts of interest

The authors declare no competing financial interests.

Data availability

The data supporting this article have been included as part of the SI.

1H NMR spectra and SEC chromatograph of SBS polymers. See DOI: **https://doi.org/10.1039/d5py00569h**.

Acknowledgements

This work was supported by contracts from the US Department of Energy, Office of Energy Efficiency and Renewable Energy (EERE), Fuel Cell Technology Office (FCTO), Award Numbers DE-EE0007647 (Program Manager: Neha Rustagi) and DE-EE0008436 (Program Manager: Donna Ho), and ARPA-E (IONICS DE-AR0000769).

References

1 S. J. Peighambardoust, S. Rowshanzamir and M. Amjadi, *Int. J. Hydrogen Energy*, 2010, **35**, 9349.
2 A. Kraytsberg and Y. Ein-Eli, *Energy Fuels*, 2014, **28**, 7303.
3 M. Carmo, D. L. Fritz, J. Mergel and D. Stolten, *Int. J. Hydrogen Energy*, 2013, **38**, 4901.
4 C. Kim, J. C. Bui, X. Luo, J. K. Cooper, A. Kusoglu, A. Z. Weber and A. T. Bell, *Nat. Energy*, 2021, **6**, 1026.
5 Y. A. Gandomi, D. S. Aaron, J. R. Houser, M. C. Daugherty, J. T. Clement, A. M. Pezeshki, T. Y. Ertugrul, D. P. Moseley and M. M. Mench, *J. Electrochem. Soc.*, 2018, **165**, A970.
6 K. Lourenssen, J. Williams, F. Ahmadpour, R. Clemmer and S. Tasnim, *J. Energy Storage*, 2019, **25**, 100844.
7 Y. Mei and C. Y. Tang, *Desalination*, 2018, **425**, 156.
8 S. Al-Amshawee, M. Y. B. M. Yunus, A. A. M. Azoddein, D. G. Hassell, I. H. Dakhil and H. A. Hasan, *Chem. Eng. J.*, 2020, **380**, 122231.
9 J. Zou, N. Han, J. Yan, Q. Feng, Y. Wang, Z. Zhao, J. Fan, L. Zeng, H. Li and H. Wang, *Electrochem. Energy Rev.*, 2020, **3**, 690.
10 M. Rhandi, M. Trégaro, F. Druart, J. Deseure and M. Chatenet, *Chin. J. Catal.*, 2020, **41**, 756.
11 M. Feng, R. Qu, Z. Wei, L. Wang, P. Sun and Z. Wang, *Sci. Rep.*, 2015, **5**, 9859.
12 M. C. Orilall and U. Wiesner, *Chem. Soc. Rev.*, 2011, **40**, 520.
13 Q. Wang, Y. Lu and N. Li, *Desalination*, 2016, **390**, 33.
14 H. Y. Hwang, H. C. Koh, J. W. Rhim and S. Y. Nam, *Desalination*, 2008, **233**, 173.
15 I. Orujalipoor, K. Polat, Y.-C. Huang, S. İde, M. Şen, U. S. Jeng, G. K. Ağçeli and N. Cihangir, *Mater. Chem. Phys.*, 2019, **225**, 399.
16 S. Adhikari, M. K. Pagels, J. Y. Jeon and C. Bae, *Polymer*, 2020, **211**, 123080.
17 S. F. Hahn, *J. Polym. Sci., Part A: Polym. Chem.*, 1992, **30**, 397.
18 A. Buonerba, V. Speranza and A. Grassi, *Macromolecules*, 2013, **46**, 778.
19 C. E. Hoyle and C. N. Bowman, *Angew. Chem., Int. Ed.*, 2010, **49**, 1540.
20 A. B. Lowe, *Polym. Chem.*, 2010, **1**, 17.
21 N. ten Brummelhuis, C. Diehl and H. Schlaad, *Macromolecules*, 2008, **41**, 9946.
22 J. Y. Jeon, D. Tian, M. K. Pagels and C. Bae, *Org. Process Res. Dev.*, 2019, **23**, 1580.
23 J. Y. Jeon, S. Park, J. Han, S. Maurya, A. D. Mohanty, D. Tian, N. Saikia, M. A. Hickner, C. Y. Ryu, M. E. Tuckerman, S. J. Paddison, Y. S. Kim and C. Bae, *Macromolecules*, 2019, **52**, 2139.
24 M. K. Pagels, S. Adhikari, R. C. Walgama, A. Singh, J. Han, D. Shin and C. Bae, *ACS Macro Lett.*, 2020, **9**, 1489.
25 T. Wang, J. Y. Jeon, J. Han, J. H. Kim, C. Bae and S. Kim, *J. Membr. Sci.*, 2020, **598**, 117665.
26 T. Wang, J. Han, K. Kim, A. Münchinger, Y. Gao, A. Farchi, Y.-K. Choe, K.-D. Kreuer, C. Bae and S. Kim, *Mater. Adv.*, 2020, **1**, 2206.
27 J. G. Petrovick, G. C. Anderson, D. I. Kushner, N. Danilovic and A. Z. Weber, *J. Electrochem. Soc.*, 2021, **168**, 056517.
28 A. Kusoglu and A. Z. Weber, *Chem. Rev.*, 2017, **117**, 987.
29 S. Turan, S. Park, C. Y. Ryu, D. Y. Ryu and C. Bae, *J. Membr. Sci.*, 2024, **700**, 122662.
30 D. Tian, S. Park, S. Jo, C. Y. Ryu, D. Y. Ryu and C. Bae, *ACS Appl. Energy Mater.*, 2024, **7**, 6209.